

ARTICLE

PIT DESIGN TAKING INTO ACCOUNT WATER LEVEL REDUCTION USING THE SOFTWARE PACKAGE MIDAS GTS NX

A.N. Sekisov¹, A.V. Varvarkina¹, D.A. Gura^{2*}, A.A. Savenko³, A.A. Shikhovtsov³

¹ Department of Construction, Kuban State Agrarian University named after I.T. Trubilin, Krasnodar, RUSSIA

² Department of Cadastre and Geo-engineering, Kuban State Technological University, Krasnodar, RUSSIA

³ Department of Technology, Organization, Economics of Construction and Real Estate Management, Kuban State Technological University, Krasnodar, RUSSIA

ABSTRACT

Using Midas GTS NX software package, the groundwater drainage is possible on the basis of needle filters and wells. This software package allows you to analyze the parameters of soil in the process of excavation. Midas GTS NX is based on the finite element method. Since this package is geotechnical one, it has a significant number of mathematical models describing the behavior of soil, depending on its physical and mechanical characteristics. One of them is the Mohr-Coulomb model. Due to this, you can get a complete picture of soil stress-strain state, to analyze and take appropriate measures.

INTRODUCTION

During the development of the pit, the groundwater level is often above the pit bottom. Thus a number of measures is required to implement artificial water drainage [1,2,3,4]. One of such methods is the device of needle-filtering units and wells.

During the implementation of the related activities, it becomes necessary to take into account the changes of developed soil physico mechanical properties [3,4,5].

The complex of calculations for the pit development is implemented in Midas GTS NX software package, taking into account dewatering. The presented complex provides the opportunity to analyze in detail the soil parameters during the excavation process. Midas GTS NX program allows you to apply the finite element method effectively. Since this complex is geotechnical, it includes a sufficient number of mathematical models that describe the behavior of soil depending on its physico mechanical characteristics [6–12]. One of them is the Mohr-Coulomb model.

METHODS AND MATERIALS

The mathematical model of Mohr-Coulomb describes the dependence of tangential stresses on the magnitude of the normal stresses applied to the material. This is due to friction inside a solid body.

The dependence of the tangential stress of the material on the magnitude of the applied normal stresses is a bilinear dependence, which is the criterion of Mohr-Coulomb strength and is described by the following formula:

$$\tau = \sigma \tan(\varphi) + c$$

where σ – the value of normal stresses,

τ – the magnitude of the tangential stresses,

c – the intersection of the strength criterion curve with τ axis,

$\tan(\varphi)$ – slope angle tangent of the strength criterion curve.

If $\varphi=0$, the Mohr-Coulomb strength criterion turns into the Tresca criterion. If $\varphi=90^\circ$, then the Mohr-Coulomb strength criterion corresponds to the Rankine viscous medium model.

For the circles of Mohr it is true that:

$$\sigma = \sigma_m - \tau_m \sin \varphi; \tau = \tau_m \cos \varphi,$$

where $\tau_m = \frac{\sigma_1 - \sigma_3}{2}$, $\sigma_m = \frac{\sigma_1 + \sigma_3}{2}$

where σ_1 – the maximum principal stress,

σ_3 – the minimum principal stress.

Therefore, the Mohr-Coulomb strength criterion can be represented as follows:

KEY WORDS

well, stress-strain state, pit, groundwater level, dewatering, finite element method.

Received: 25 Oct 2018
Accepted: 21 Dec 2018
Published: 10 Jan 2019

*Corresponding Author

Email:
gda-kuban@mail.ru

$$\tau_m = \sigma_m \sin \varphi + c \cos \varphi$$

This type of Mohr-Coulomb strength criterion corresponds to the fracture on a plane parallel to the direction of the main stress σ_2 .

The Mohr-Coulomb strength criterion is used to analyze the bearing capacity of soil massifs.

During loading soils work mainly on surface shear with the lowest bearing capacity. Therefore, shear strength is the defining strength characteristic for soils.

The destruction occurs at the moment when the magnitude of the shear (tangential) stress reaches the ultimate soil strength at shear. Therefore, the relationship between normal shear stresses is the criterion of strength for soils.

Let's consider the solution to this problem by example.

There is the evidence of the construction site engineering-geological profile [Fig. 1].

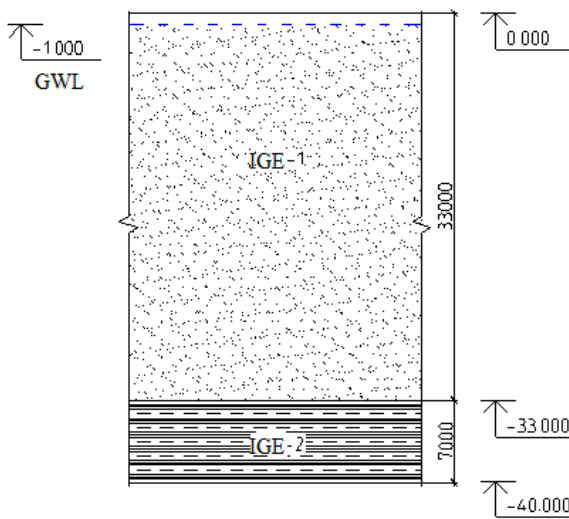


Fig. 1: Engineering-geological section.

The geotechnical data of the construction site is presented below [Table 1].

Table 1: Geotechnical data

Soil name	Specific soil adhesion with, kPa	The angle of internal friction, φ , deg.	The modulus of the total strain E, MPa	The specific weight of soil particles γ_w	The specific weight of soil γ_w kN/m ³	Poisson's ratio μ	Layer thickness, m
EGE 1	1	35	30×10^6	21	17	0.3	33
EGE 2	49	24	42×10^6	21	19,5	0,32	7

During the excavation development, HYUNDAI R330LC-9A crawler excavator was used. The loading was carried out via MAN TGA 33.350 6X4 BB-WW dump truck with a bucket capacity of 15 m³ [Fig. 2].

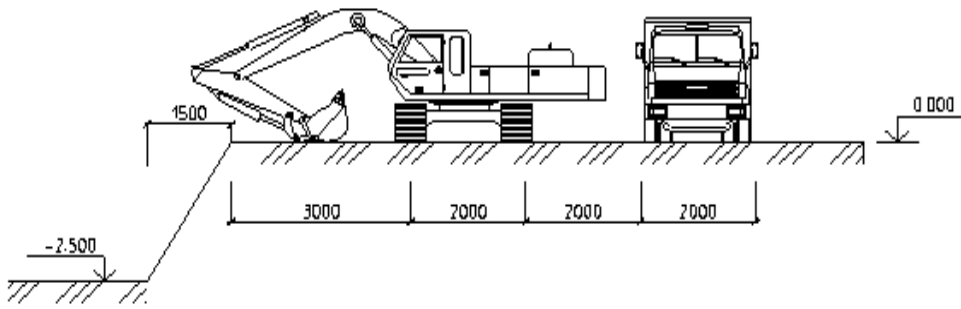


Fig. 2: Pit development scheme using construction machines and mechanisms.

The actual loads and impacts during the pit development at the construction site are presented below [Table 2].

Table 2: Loads and Impacts

Load name	Meas. Un.	Rated value	Safety factor	Design value
Constant				
Net weight of the 1st layer of soil (sand)	t/m ³	1.7	1,1	1,87
Net weight of the 2nd layer of soil (clay)	t/m ³	1.95	1,1	2,15
Temporal load				
Excavator	kN	75	-	75
Dump truck	kN	75	-	75

The design scheme of the excavation at the construction site is presented below [Fig. 3].

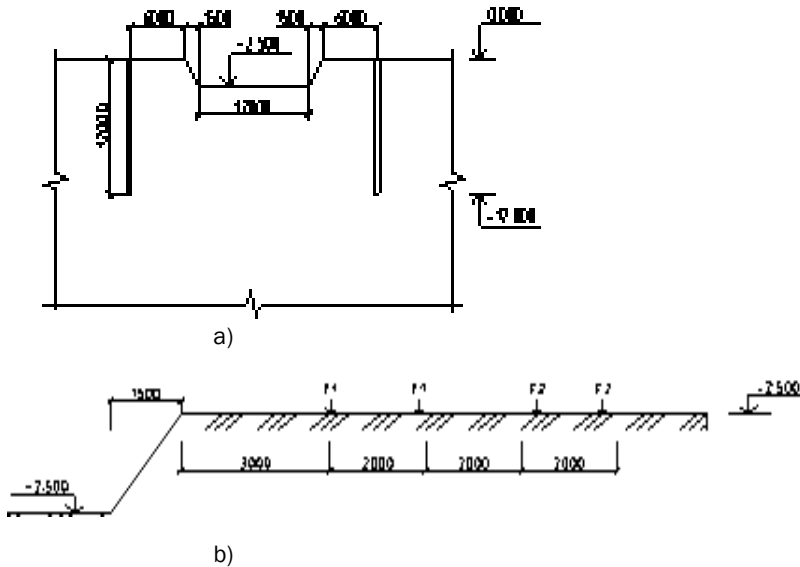


Fig. 3: The design scheme of the excavation design: a) the design of wells, b) the load from the construction machines and mechanisms.

The generated finite element model in Midas GTS NX software [Fig. 4].

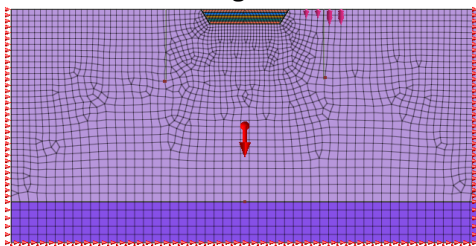


Fig. 4: Finite-element model.

[Fig. 5-13] demonstrate iso-fields at different stages of calculation (type of loading), which we consider in this problem.

The first stage is filtering, which we determine for the given soil conditions.

At the second stage, the stress-strain state (SSS) of soil strata is considered.

The third stage is characterized by the appearance of an excavator at a construction site for the development of soil (the load from an excavator).

The next calculation step is the accounting for the separation of the first excavation and its loading into a dump truck (a dump truck arrived at the construction site for excavated soil loading into it).

Then the separation of the second excavation and the loading of the excavated soil into the dump truck takes place. The truck has already been emptied from the first part of soil (took it to another part of the construction site where filling is required).

Then the calculation stage takes place with the separation of the third excavation and the loading of soil from the third excavation into the dump truck.

A similar situation is observed during the step 7 of the computational model, where the separation of the excavation 4 and the loading of the fourth soil into the dump truck takes place.

Step 8, the final one, the separation of the excavation 5 and the loading of the remaining soil in the dump truck.

During the current model calculation, the following values were obtained:

a) initial filtration [Fig. 5].

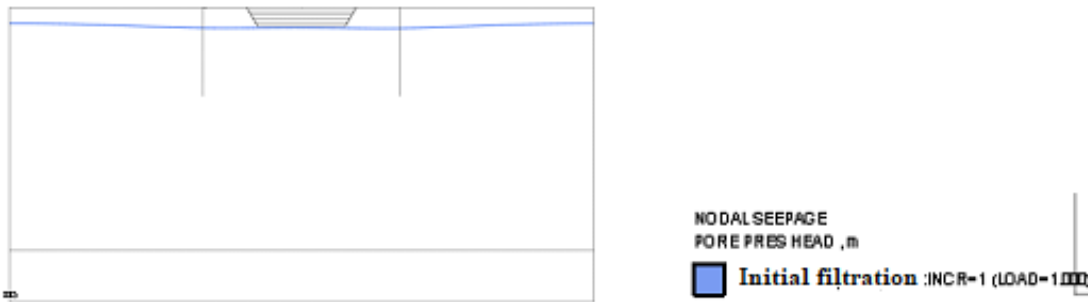


Fig. 5: Initial filtration.

The line shows the level of filtration in a given soil massif after water-lowering using a well device.

b) pore pressure, after the excavator arrival at the construction site [Fig. 6].



Fig. 6: Pore pressure.

The pore pressure isoline represents the calculation results in the software after the excavator arrival at the construction site to develop the excavation.

c) deformations (maximum and minimum) arising from the own weight of the excavator [Fig. 7].

The maximum and the minimum values of deformations along Y axis that occur during the excavation of the upper soil layer by the excavator [Fig. 7].

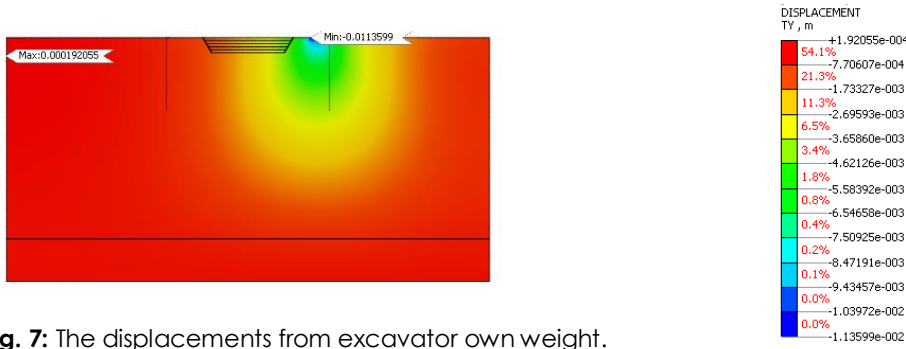


Fig. 7: The displacements from excavator own weight.

d) the deformations during the development of the first soil layer [Fig. 8].

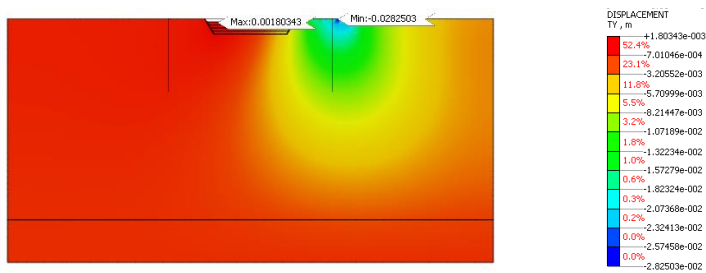


Fig. 8: Displacements from the excavator weight during the first soil layer development.

e) deformations during the development of the second layer of soil [Fig. 9].

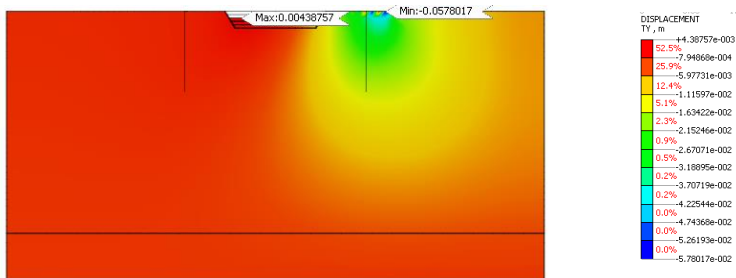


Fig. 9: The displacements from excavator and dump truck weight during the second soil layer development.

f) the deformations during the development of the third soil layer [Fig. 10].

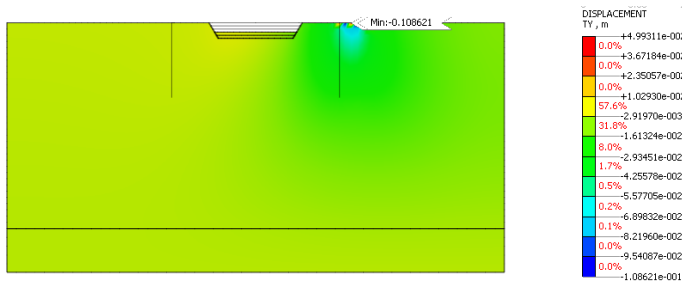


Fig. 10: The deformations from excavator and dump truck weight during the third layer of soil development.

g) The deformations during the fourth layer of soil development [Fig. 11].

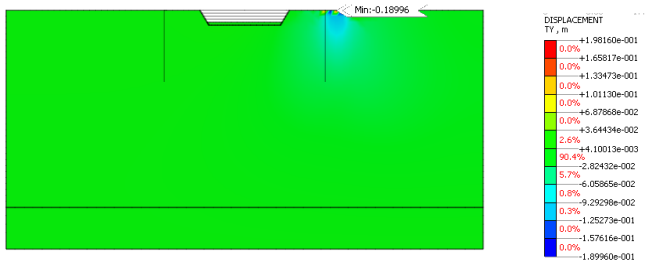


Fig. 11: Deformations from excavator and dump truck weight during the development of the fourth layer of soil.

h) deformations during the development of the fifth soil layer [Fig. 12].



Fig. 12: Deformations from excavator and dump truck weight during the development of the fifth layer of soil.

i) The stresses in XY plane [Fig. 13].

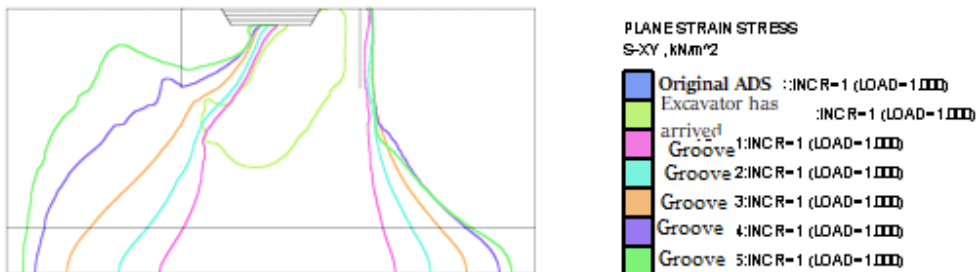


Fig. 13: The stresses in XY plane XY.

Iso fields display the stress distribution from the corresponding loads [Table 3].

Table 3: Calculation results

Load type	Pore pressure/ (stress), kPa/ (kN/m ²)		Movement, m		Stress, kN/m ²			
	Max	Min	Max	Min	Max		Min	
					XY	Y	XY	Y
1	382,5	-27,4	-	-	-	-	-	-
2	1,0	-382,5	-	-	1,3	-3,5	-1,2	-440,1
3	1,0	-382,5	1,9×10 ⁻⁴	-1,1×10 ⁻²	10,0	-0,5	-11,0	-442,6
4	1,0	-382,5	1,8×10 ⁻³	-2,8×10 ⁻²	23,3	4,9	-16,0	-447,7
5	1,0	-382,5	4,4×10 ⁻³	-5,8×10 ⁻²	37,4	55,3	-33,3	-452,4
6	1,0	-382,5	5,2×10 ⁻²	-1,1×10 ⁻¹	59,7	147,3	-56,8	-796,5
7	1,0	-382,5	0,2	-0,2	107,4	324,0	-84,4	-1269
8	1,0	-382,5	0,5	-0,3	148,0	436,6	-137,1	-1850

Loading type: 1 - filtration; 2 - stress-strain state (SSS); 3 - the load from excavator; 4 - the separation of excavation 1 and the loading of the first soil into the dump truck; 5 - the separation of excavation 2 and

the loading of the second soil into the dump truck; 6 - the separation of the excavation 3 and the loading of the third soil into the dump truck; 7 - the separation of excavation 4 and the loading of the fourth soil into the dump truck; 8 - the separation of the excavation 5 and the loading the remaining soil into the dump truck.

Having analyzed the results of the calculations presented in [Table 3], let's develop the dependency graphs, thanks to which it will be possible to understand how the stress-strain state of soil depends on soil saturation with water. Analyzing [Fig. 14-16] it is possible to trace the physico mechanical changes in soil by stages.

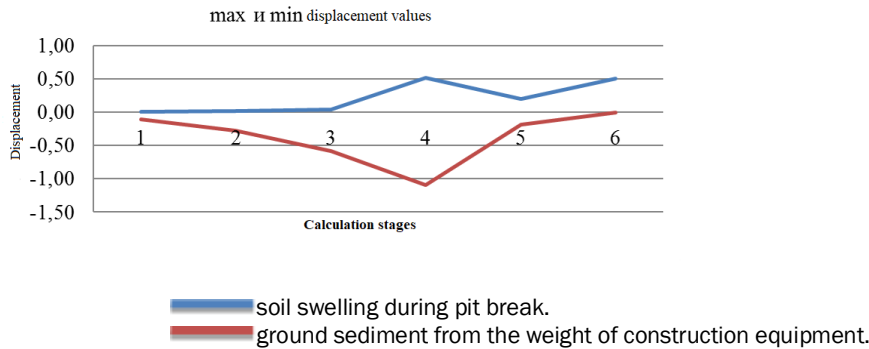


Fig. 14: The graph of maximum and minimum displacements.

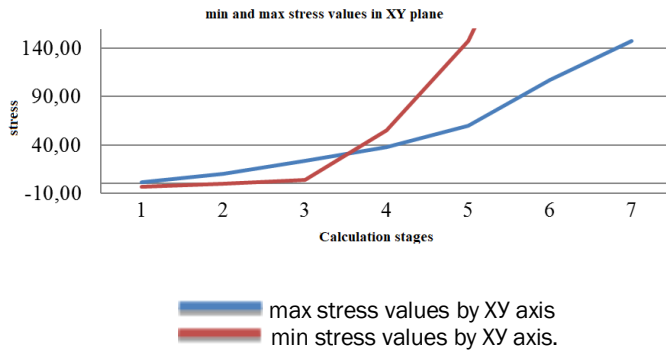


Fig. 15: The graph of maximal and minimal stresses.

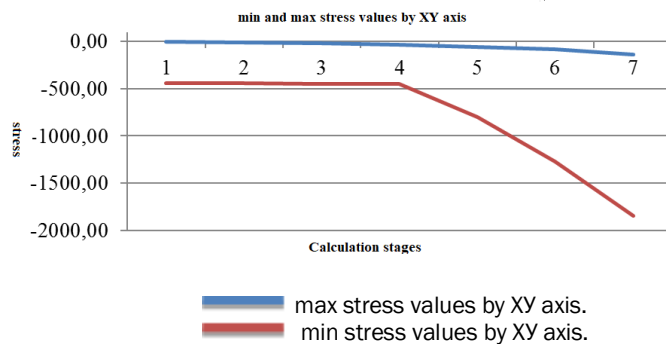


Fig. 16: The graph of maximum and minimum stresses along Y axis.

RESULTS

Thus, under the action of a load applied to the base by construction machines, the stress state arises in soil, which causes the development of deformations leading to the displacement (the settlement) of the soil surface.

The analysis of soil problem solution results showed that SSS significantly depends on the degree of soil saturation with water. At the end of the primary (filtration) consolidation, the pore pressure at all stages makes 1, hence the sediment is caused solely by the shear deformations of the soil skeleton. Soil is compacted with water lowering.

This task, which was calculated in Midas GTS NX software package, can be used during drainage calculation, the determination of underground water supply source debit, the calculation of structure sediments over time, an artificial lowering of groundwater level and the digging out of pits.

CONCLUSION

The scientific novelty of the study is in a new multifactorial approach for this problem solution, namely: the determination of the mathematical model for the soil conditions of the construction site, the selection of machines and mechanisms for pit excavation, the arrangement of water-reducing plants and the determination of their characteristics and step-by-step calculation in Midas GTS NX.

Only when the multifactorial nature of the problem and the availability of reliable data on the foundation soils are taken into account one can carry out the measures for water lowering successfully.

CONFLICT OF INTEREST

There is no conflict of interest.

ACKNOWLEDGEMENTS

None

FINANCIAL DISCLOSURE

None

REFERENCES

- [1] Degtyareva OG. [2016] Using CAE-systems for solving engineering problems, Scientific support of the agro-industrial complex. Collection of articles based on the materials of the 71st Scientific and Practical Conference of Teachers on the basis of research in 2015. Krasnodar: KubSAU, 2016: 462-463.
- [2] Degtyareva OG. [2014] Features of the analysis of the state of a building under construction in complex hydrogeological conditions of the city of Sochi", Polythematic network electronic scientific journal of the Kuban State Agrarian University, Krasnodar: Kuban State Agrarian University, 7: 1-25.
- [3] Degtyarev VG, et al. [2018] Modeling of the Building by Numerical Methods at Assessment of the Technical Condition of Structures. International conference on Construction and Architecture: theory and practice of industry development (CATPID-2018). Trans Tech Publications, Switzerland, 931: 141-147.
- [4] Degtyareva OG, et al. [2018] The Calculation of a Drain Seasonal Regulation Reservoir Volume Probability. International conference on Construction and Architecture: theory and practice of industry development (CATPID-2018). Trans Tech Publications, Switzerland, 931: 991-995.
- [5] Degtyarev VG, et al. [2018] The Foundation Pit Deep Site Ground State Design Modelling Process. International conference on Construction and Architecture: theory and practice of industry development (CATPID-2018). Trans Tech Publications, Switzerland, 931: 396-404.
- [6] Nehaj R, et al. [2017] Algorithm of composing the schedule of construction and installation works. IOP Conference Series: Earth and Environmental Science, 90 (1):1-8.
- [7] Sekisov AN, et al. [2018] Development of the Methods Improving the Production Costs Formation Process, International conference on Construction and Architecture: theory and practice of industry development (CATPID-2018). Trans Tech Publications, Switzerland, 931:1210-1213.
- [8] Litvinov SV, et al. [2018] Buckling of Glass Reinforced Plastic Rods of Variable Rigidity. International conference on Construction and Architecture: theory and practice of industry development (CATPID-2018). Trans Tech Publications, Switzerland, 931: 133-140.
- [9] Degtyarev GV, et al. [2018] Numerical modeling of condition of the bridge structure based on the results of national surveys. International Journal of Engineering & Technology, 7(2.13),226-230.
- [10] Yazyev BM, et al. [2018] The Definition of a Critical Deflection of Compressed Rods with the Creep by the Method of Bubnov-Galerkin. International conference on Construction and Architecture: theory and practice of industry development (CATPID-2018). Trans Tech Publications, Switzerland, 931: 127-132.
- [11] Gura DA, et al. [2017] Application of inertial measuring unit in air navigation for ALS and DAP // Journal of Fundamental and Applied Sciences, 9(1S): 732-741.
- [12] Kuzyakina MV, et al. [2018] Experimental analysis of srtm model by image processing and geostatistical methods, International Journal of Engineering and Technology(UAE). 7(4.7): 250-253.